

# Calculation of yield stresses and plastic strain ratios

DONG NYUNG LEE, INSOO KIM

*Department of Metallurgical Engineering, Seoul National University, Seoul 151, Korea*

KYU HWAN OH

*Division of Materials Engineering, Korea Advanced Institute of Science and Technology, Seoul 131, Korea*

Yield stresses and plastic strain ratios of aluminium, copper, brass and steel sheets having various textures, which are characterized by the orientation distribution functions, have been calculated as a function of angle to the rolling direction using the Bunge method based on Taylor's minimum energy theory and another method suggested by the present authors. The calculated results are compared with the measured ones. For steels, the two methods yield almost identical yield stress results. The Bunge method yields higher average plastic strain ratios than the measured data, while their variation with the angle to the rolling direction agrees very well with the measured values. The plastic strain ratios calculated by the second method are in very good agreement with the measured data in their average values but show smaller variations with the angle to the rolling direction than the measured. Therefore, combination of the two methods can yield very good agreement between calculated and measured plastic strain ratios. For the fcc metals, the calculated yield stresses and plastic strain ratios are in good agreement with measured data, regardless of the calculation method.

## 1. Introduction

Deep drawability is closely related to the plastic strain ratio or  $R$ , which is defined as the ratio of true strains in the width and thickness directions under tension. For planar isotropic sheets, a higher  $R$  value implies higher resistance to thinning in the thickness direction, resulting in a higher limiting drawing ratio. Theoretical works on this have been undertaken by Whiteley [1] and Lee [2, 3]. The variation of  $R$  with tensile direction is associated with earing behaviour in deep drawing. Earing occurs along the directions of higher  $R$  values.

It is well known that sheet anisotropy is closely related to sheet texture. A method has been proposed by Hosford and Backofen [4] for the prediction of  $R$  and yield stress as a function of sheet texture based on finding the combination of slip systems that minimizes the work per unit volume required to produce a given strain [5]. Bunge *et al.* [6] refined this method using a sheet texture described by the orientation distribution function.

Another method was advanced by Lee *et al.* for the prediction of the  $R$  value [7] and the yield stress [8], which will be explained in the next section. In the previous works [7, 8], the volume fraction of a texture component was estimated on the basis of peak intensity in the pole figure, because the orientation distribution function was not known. The purpose of this paper is to compare the measured  $R$  values and yield stresses of fcc and bcc sheet specimens with those calculated by the two methods using measured orientation distribution functions.

## 2. Calculation methods

### 2.1. The Bunge method [6]

Fig. 1 shows the plastic strain tensor with respect to the specimen coordinate system. The strain may be written as

$$d\varepsilon_{ij} = d\eta \begin{pmatrix} 1 & 0 & 0 \\ 0 & -q & 0 \\ 0 & 0 & -(1-q) \end{pmatrix} \quad (1)$$

where  $d\eta$  is the absolute value of a strain increment and  $q$  is the contraction ratio, that is, the ratio of the width strain to the longitudinal strain. The ratio,  $q$ , can be related to the plastic strain ratio or the Lankford parameter,  $R$ , that is, the ratio of the width strain to the thickness strain as follows

$$q = R/(1 + R) \quad (2)$$

The deformation work for the strain to take place can be expressed as

$$dA = d\eta\tau_0 M(g, q) \quad (3)$$

where  $\tau_0$  is the critical resolved shear stress in the slip systems and  $M$  is a geometrical factor which depends on the orientation  $g$  of the crystal with respect to the principal strain axes and on the contraction ratio. If the factor  $M$  is evaluated based on Taylor's minimum work theory [5], it becomes the Taylor factor. The deformation work and the Taylor factor for a polycrystalline specimen may be evaluated by averaging

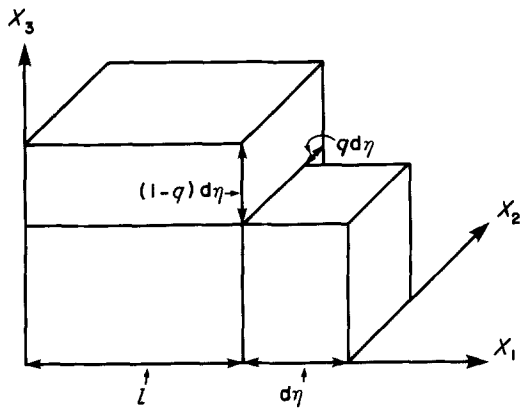


Figure 1 General deformation in the principal axis representation.

those for single crystals

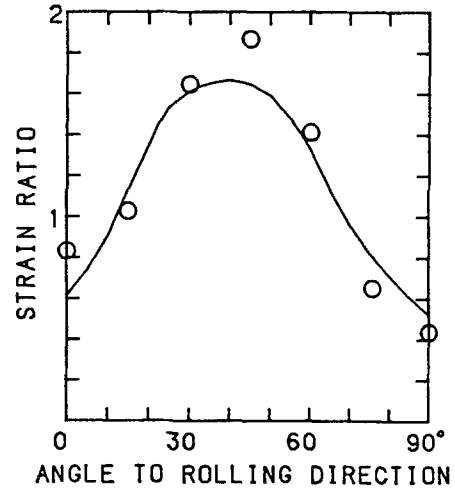
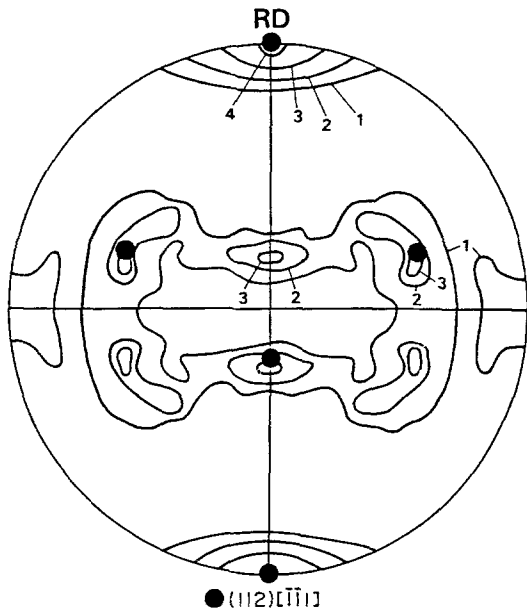
$$d\bar{A}_{\min} = \tau_0 \bar{M}(q) d\eta \quad (4)$$

$$\bar{M}(q) = \phi M(q, g) f(g) dg \quad (5)$$

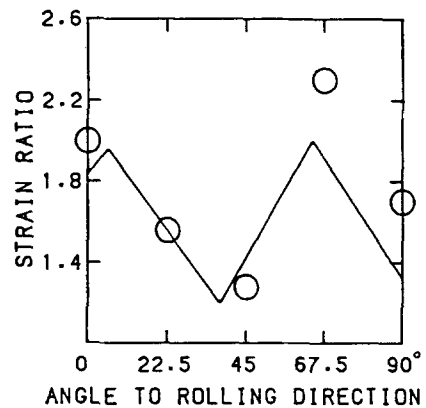
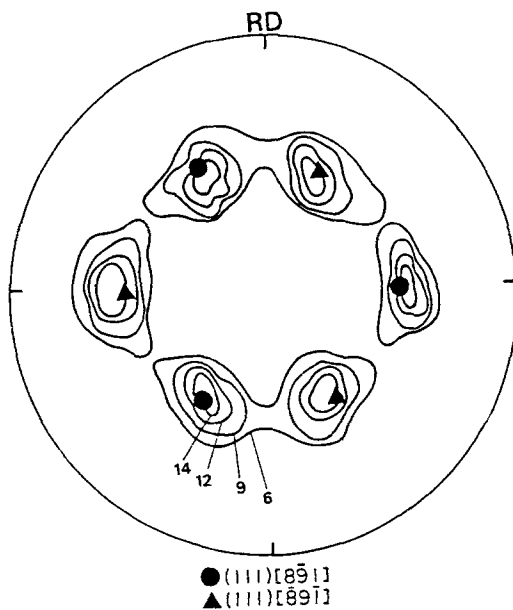
where  $f(g)$  is the orientation distribution function (ODF) and is defined by

$$\frac{\Delta V(g)}{V} = f(g) dg \quad (6)$$

Here  $\Delta V(g)$  is the volume of all the crystallites having orientations in the range from  $g$  to  $g + \Delta g$  and  $V$  is the volume of the whole sample. The ODF characterizes the texture of the sample and is unity in the case of random orientation distribution.



(a)



(b)

Figure 2  $R$  as a function of tensile direction for (a) copper and (b) 444 stainless steel sheets: (O) measured; (—) calculated based on the (111) pole figure of the copper sheet and (001) pole figure of the 444 stainless steel sheet [7].

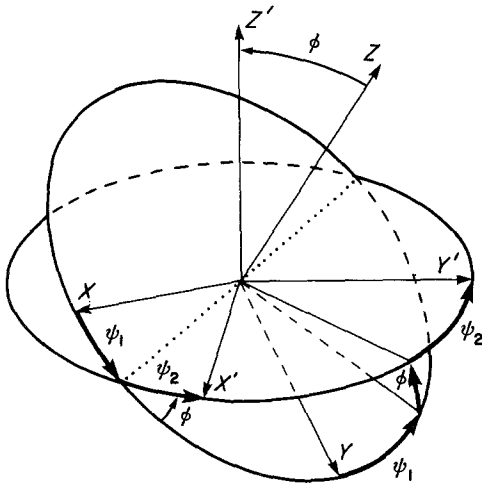


Figure 3 Definition of the Euler angles.

Bunge developed  $f(g)$  and  $M(q, g)$  into a series of generalized spherical harmonics, as follows

$$f(g) = \sum_{l=0}^{\infty} \sum_{\mu=1}^{M(l)} \sum_{\nu=1}^{N(l)} C^{\mu\nu} \dot{T}^{\mu\nu}(g) \quad (7)$$

$$M(q, g) = \sum_{l=0}^{\infty} \sum_{\mu=1}^{M(l)} \sum_{\nu=1}^{N(l)} m_l^{\mu\nu}(q) \ddot{T}_l^{\mu\nu}(g) \quad (8)$$

Substitution of Equations 7 and 8 into Equation 5 gives us

$$\bar{M}(q) = \sum_{l=0}^{\infty} \sum_{\mu=1}^{M(l)} \sum_{\nu=1}^{N(l)} \frac{1}{2l+1} m_l^{\mu\nu}(q) C_l^{\mu\nu} \quad (9)$$

$$\begin{pmatrix} d\varepsilon_2 \\ d\varepsilon_3 \\ d\varepsilon_4 \\ d\varepsilon_5 \\ d\varepsilon_6 \end{pmatrix} = \begin{pmatrix} (n_2 b_2)_1 & (n_2 b_2)_2 & (n_2 b_2)_3 & (n_2 b_2)_4 & (n_2 b_2)_5 \\ (n_3 b_3)_1 & (n_3 b_3)_2 & (n_3 b_3)_3 & (n_3 b_3)_4 & (n_3 b_3)_5 \\ (n_2 b_3 + n_3 b_2)_1 & (n_2 b_3 + n_3 b_2)_2 & (n_2 b_3 + n_3 b_2)_3 & (n_2 b_3 + n_3 b_2)_4 & (n_2 b_3 + n_3 b_2)_5 \\ (n_1 b_3 + n_3 b_1)_1 & (n_1 b_3 + n_3 b_1)_2 & (n_1 b_3 + n_3 b_1)_3 & (n_1 b_3 + n_3 b_1)_4 & (n_1 b_3 + n_3 b_1)_5 \\ (n_1 b_2 + n_2 b_1)_1 & (n_1 b_2 + n_2 b_1)_2 & (n_1 b_2 + n_2 b_1)_3 & (n_1 b_2 + n_2 b_1)_4 & (n_1 b_2 + n_2 b_1)_5 \end{pmatrix} \begin{pmatrix} d\gamma_1 \\ d\gamma_2 \\ d\gamma_3 \\ d\gamma_4 \\ d\gamma_5 \end{pmatrix} \quad (15)$$

Numerical values of the coefficients  $m_l^{\mu\nu}(q)$  have been published and  $C_l^{\mu\nu}$  can be calculated from measured pole data.

The mean Taylor factor along the angle,  $\alpha$ , to the rolling direction of a rolled sheet specimen can be expressed as

$$\bar{M}(q)_\alpha = \sum_{l=0}^{10} \sum_{\mu=1}^{M(l)} \sum_{\nu=1}^{N(l)} \frac{1}{2l+1} m_l^{\mu\nu}(q) C_l^{\mu\nu} \cos [2(\nu-1)\alpha] \quad (10)$$

The  $R$  value or the Langford parameter along the direction of the angle,  $\alpha$ , to the rolling direction,  $R(\alpha)$ , is calculated using  $q$  which minimizes  $\bar{M}(q)_\alpha$ , that is,

$$\frac{d\bar{M}(q)_\alpha}{dq} = 0, \quad q = q_{\min}(\alpha) \quad (11)$$

where  $q_{\min}(\alpha)$  is the value of  $q$  which minimize  $\bar{M}(q)_\alpha$ . It follows from Equation 1 that

$$R(\alpha) = q_{\min}(\alpha)/[1 - q_{\min}(\alpha)] \quad (12)$$

The yield stress along the direction of  $\alpha$  to the rolling direction is from Equation 4 given by

$$\sigma_y(\alpha) = \tau_0 \bar{M}[q_{\min}(\alpha)] \quad (13)$$

## 2.2. The second method

Suppose that we have several slip systems operating at the same time, with a shear strain of  $d\gamma_j$  on the  $j$ th slip system. Each component of the total strain is obtained simply by adding the corresponding contributions from all the systems, provided that these strains are small.

$$d\varepsilon_i = E_{ij} d\gamma_j \quad (14)$$

An arbitrary strain with no change in volume can be specified by five  $d\varepsilon_i$ s, and one of the normal strains, say  $d\varepsilon_1$ , is redundant, because  $d\varepsilon_1 + d\varepsilon_2 + d\varepsilon_3 = 0$  [5]. Equation 14 means that arbitrary values of  $d\varepsilon_2, \dots, d\varepsilon_6$  can be achieved by shear strains  $d\gamma_j$  on appropriate slip systems. Equation 14 can be written out in full as (for example, see [9])

where  $d\varepsilon_2 = d\varepsilon_{22}$ ,  $d\varepsilon_3 = d\varepsilon_{33}$ ,  $d\varepsilon_4 = 2d\varepsilon_{23}$ ,  $d\varepsilon_5 = 2d\varepsilon_{13}$ , and  $d\varepsilon_6 = 2d\varepsilon_{12}$ ;  $n_1, n_2$ , and  $n_3$  are the directional cosines of a vector normal to the slip plane;  $b_1, b_2$  and  $b_3$  are the directional cosines of a vector in the slip direction, and the subscript on the right side of parenthesis indicates the slip system referred to.

When a single crystal is subjected to the uniaxial tension in the direction of the  $x_1$  axis, it is not guaranteed that  $d\varepsilon_4, d\varepsilon_5$  and  $d\varepsilon_6$  will all be zero.

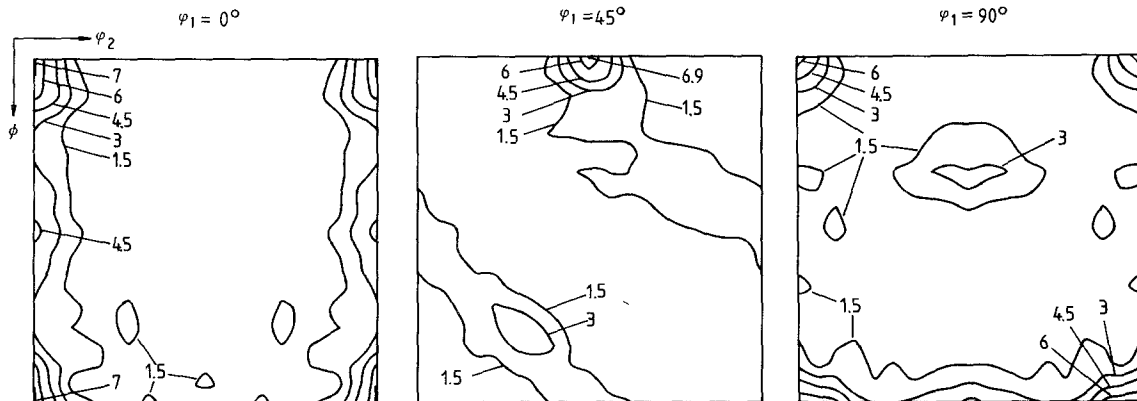


Figure 4 The ODF for specimen Al-90 in  $\psi_1$ -sections.

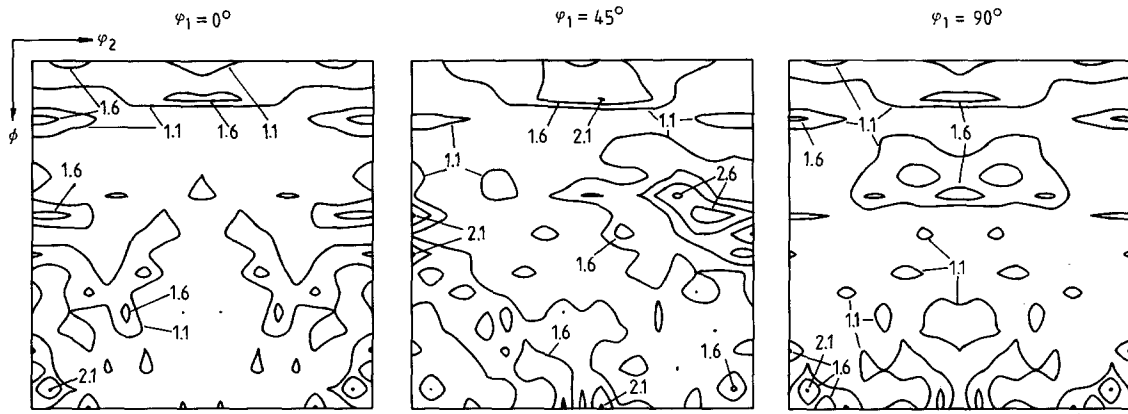


Figure 5 The ODF for specimen brass-70 in  $\psi_1$ -sections.

A polycrystal sheet which has a well-developed texture may be approximated by a single crystal. When the sheet specimen is subjected to the uniaxial tension in the direction of the  $x_1$  axis,  $d\varepsilon_{22}$  and  $d\varepsilon_{33}$  are expected to be principal strains, that is,  $d\varepsilon_4 = d\varepsilon_5 = d\varepsilon_6 = 0$ . It follows from Equation 15 that the plastic strain ratio or  $R$  of the specimen may be expressed as

$$R = \frac{d\varepsilon_{22}}{d\varepsilon_{33}} = \frac{\sum_{i=1}^5 (n_2 b_2)_i d\gamma_i}{\sum_{i=1}^5 (n_3 b_3)_i d\gamma_i} \quad (16)$$

If only one slip system operates, then Equation 16 reduces to

$$R = \frac{n_2 b_2}{n_3 b_3} \quad (17)$$

Let  $w$ ,  $t$ ,  $d$  and  $p$  be unit vectors along the width, thickness and slip directions and the direction normal to the slip plane, respectively. Then Equation 17 can be rewritten by

$$R = \frac{|(w \cdot p)(w \cdot d)|}{|(t \cdot p)(t \cdot d)|} \quad (18)$$

because  $n_2 = w \cdot p$ ,  $b_2 = w \cdot d$ ,  $n_3 = t \cdot p$  and  $b_3 = t \cdot d$ . Equation 18 has been used to calculate  $R$  using ideal textures which approximate measured textures [10, 11]. In order for Equation 18 to be used, it is necessary to choose appropriate slip systems. A slip system with the largest Schmid factor from the applied tensile stress, or several slip systems with larger Schmid factors were used [10, 11].

Recently, Lee suggested using the following equation [7].

$$R = \frac{d\varepsilon_w}{d\varepsilon_t} = \frac{\sum_i (|(w \cdot p)(w \cdot d)|_i S_i)}{\sum_i (|(t \cdot p)(t \cdot d)|_i S_i)} \quad (19)$$

where  $\Sigma$  indicates the summation of the total slip systems and  $S$  is the Schmid factor of the corresponding slip systems which can be explicitly expressed as

$$S_i = |(l \cdot p)(l \cdot d)|_i \quad (20)$$

with  $l$  being the unit vector along the tensile direction. Equation 19 means that all the slip systems contribute to the deformation but their contributions are proportional to their Schmid factors or that  $d\gamma_i$  in Equation 16 is linearly proportional to  $S_i$  apart from Equation 16 requiring only five slip systems. In fact, the number of slip systems, on which the Schmid factors have the first to the fifth largest magnitude, can exceed five. Therefore, it is convenient to consider all the slip systems whose contribution is left to the Schmid factor.

For a sheet specimen having texture  $(R_1 R_2 R_3)$  ( $A_1 A_2 A_3$ ) subjected to tension along the angle,  $\alpha$ , to the rolling direction and for a slip system of  $(P_1 P_2 P_3)$  ( $D_1 D_2 D_3$ ), the unit vectors in Equations 19 and 20 are given by [7]

$$p = (p_1, p_2, p_3) = (P_1/|P|, P_2/|P|, P_3/|P|)$$

$$\text{with } |P| = (P_1^2 + P_2^2 + P_3^2)^{1/2}$$

$$d = (d_1, d_2, d_3) = (D_1/|D|, D_2/|D|, D_3/|D|)$$

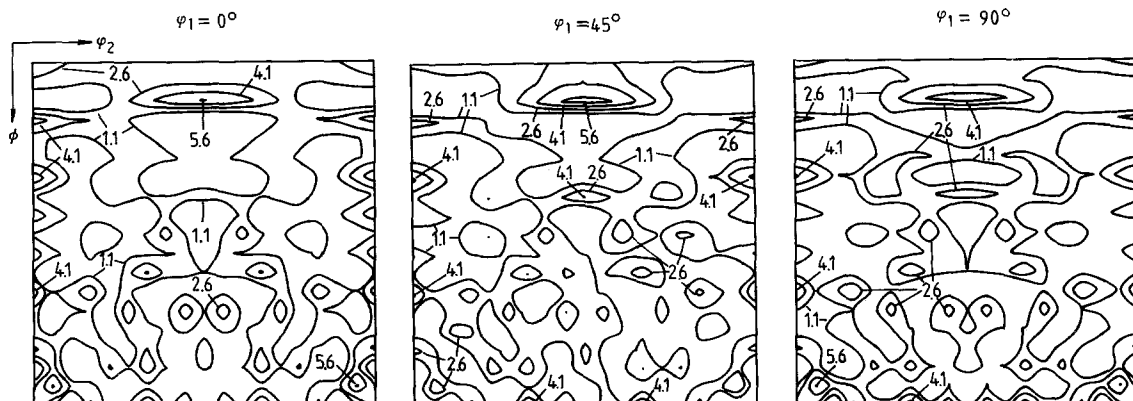


Figure 6 The ODF for specimen Cu-70 in  $\psi_1$ -sections.

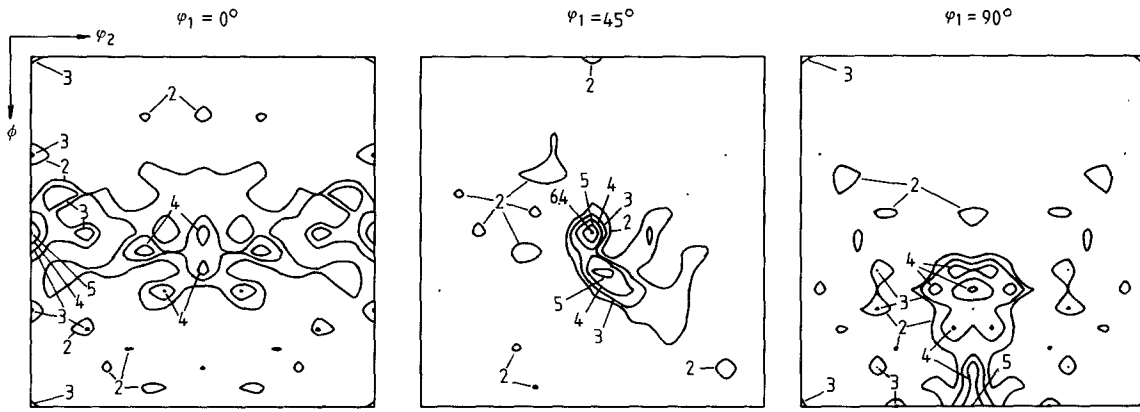


Figure 7 The ODF for specimen steel A-30A in  $\psi_1$ -sections.

with  $|D| = (D_1^2 + D_2^2 + D_3^2)^{1/2}$

$$\mathbf{t} = (r_1, r_2, r_3) = (R_1/|R|, R_2/|R|, R_3/|R|)$$

with  $|R| = (R_1^2 + R_2^2 + R_3^2)^{1/2}$

$$\mathbf{b} = (b_1, b_2, b_3)$$

$$\begin{aligned} &= (-a_1 \sin \alpha + (a_2 r_3 - a_3 r_2) \cos \alpha, \\ &\quad -a_2 \sin \alpha + (a_3 r_1 - a_1 r_3) \cos \alpha, \\ &\quad -a_3 \sin \alpha + (a_1 r_2 - a_2 r_1) \cos \alpha) \end{aligned}$$

where

$$(a_1, a_2, a_3) = (A_1/|A|, A_2/|A|, A_3/|A|)$$

with  $|A| = (A_1^2 + A_2^2 + A_3^2)^{1/2}$

$$\begin{aligned} \mathbf{l} = (l_1, l_2, l_3) = &(a_1 \cos \alpha + (a_2 r_3 - a_3 r_2) \sin \alpha, \\ &a_2 \cos \alpha + (a_3 r_1 - a_1 r_3) \sin \alpha, \\ &a_3 \cos \alpha + (a_1 r_2 - a_2 r_1) \sin \alpha) \end{aligned}$$

Equation 19 yielded satisfactory results as shown in Fig 2, where sheet texture was approximated by single ideal texture.

For a sheet specimen being approximated by more than one ideal texture, the following equation has been suggested by Lee and Oh [7]

$$R = \frac{d\epsilon_w}{d\epsilon_t} = \frac{\sum_i d\epsilon_{wi} V_i}{\sum_i d\epsilon_{ti} V_i} = \frac{\int_v d\epsilon_w(g) \cdot f(g) dg}{\int_v d\epsilon_t(g) f(g) dg} \quad (21)$$

where  $d\epsilon_{wi}$ ,  $d\epsilon_{ti}$  and  $V_i$  are, respectively, the strains in the width and thickness directions and the volume

fraction of texture component  $i$ ;  $g$  and  $f(g)$  are the orientation and the orientation distribution function. It is difficult to obtain  $V_i$  from a single pole figure. A way of obtaining approximate values of  $V_i$  has been proposed by Lee and Oh [7].

The yield stress of a single crystal having one slip system can be described by the Schmid law.

$$\sigma_y = \tau_0/S \quad (22)$$

where  $\tau_0$  is the critical resolved shear stress and  $S$  is the Schmid factor. For a polycrystalline specimen, even though its texture may be approximated by an ideal texture, only one slip system can be expected not to operate in order for 0.2% plastic deformation to take place, because of grain boundaries. Therefore, Lee [8] suggested the following relation for 0.2% offset yield strength of a specimen whose texture may be approximated by an ideal texture

$$\sigma_y = k \left/ \sum_{i=1}^n S_i \right. \quad (23)$$

where  $k$  is a constant,  $S_i$  the Schmid factor on slip system  $i$  (Equation 20) and  $n$  the total number of slip systems, for example, 12 in fcc metals. In general, the yield stress of a specimen may be as in Equation 21 for the  $R$  value expressed as

$$\sigma_y = \sum_j V_j \sigma_{yj} = \int_v \sigma_y(g) f(g) dg \quad (24)$$

Suppose that the orientation distribution function of a specimen is known. The orientation is often defined by Euler angles  $\psi_1$ ,  $\phi$  and  $\psi_2$  (Fig. 3). For

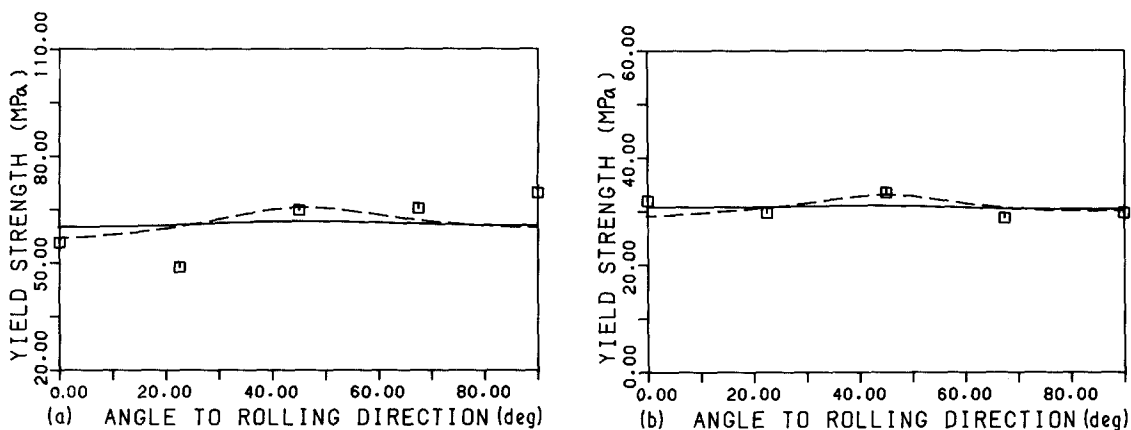


Figure 8 The yield strength as a function of tensile direction for (a) Al-0 and (b) Al-90 specimens.

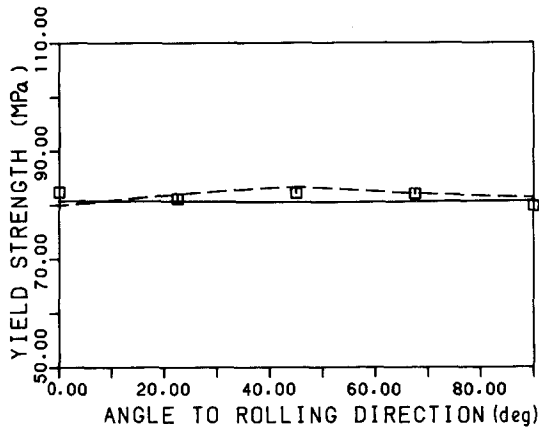


Figure 9 The yield strength as a function of tensile direction for specimen brass-0. (—) Bunge [6], (---) Lee [8], (□) measured.

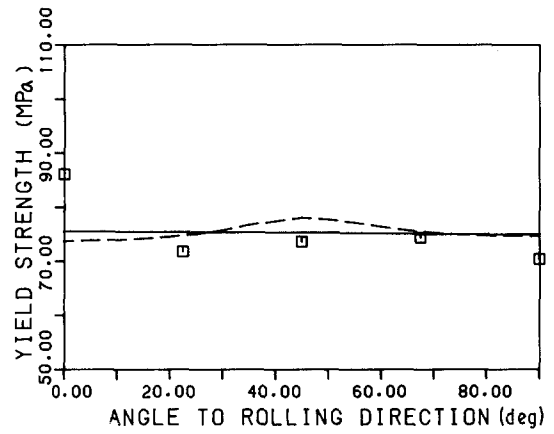


Figure 10 The yield strength as a function of tensile direction for specimen Cu-70. (—) Bunge [6], (---) Lee [8], (□) measured.

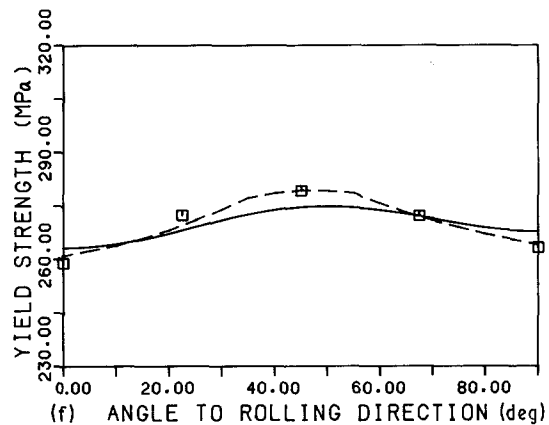
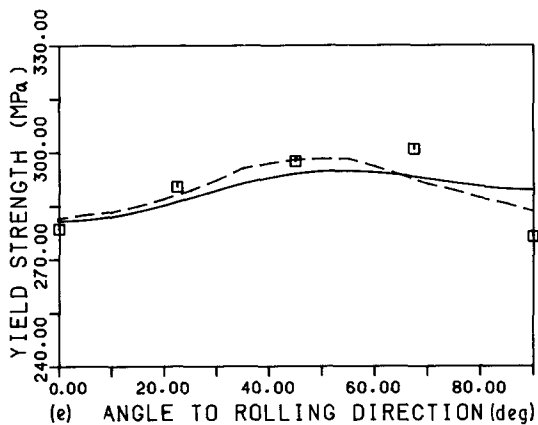
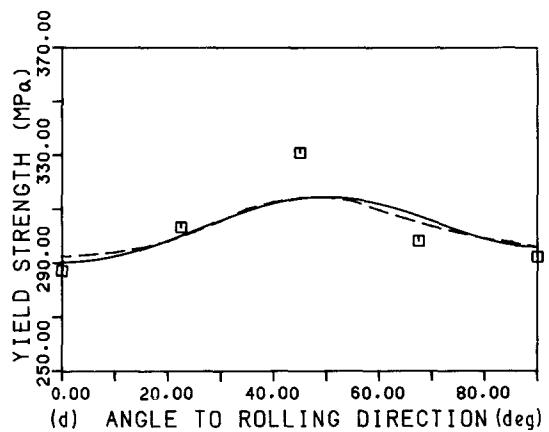
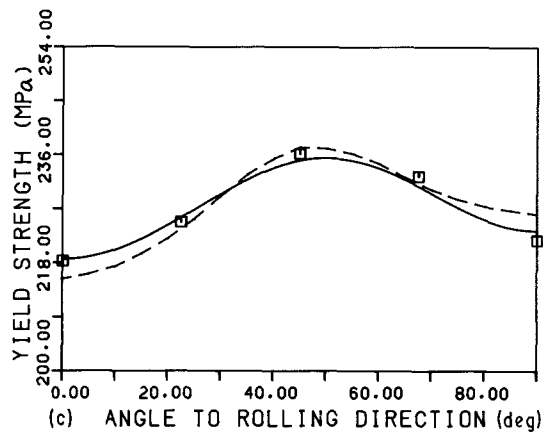
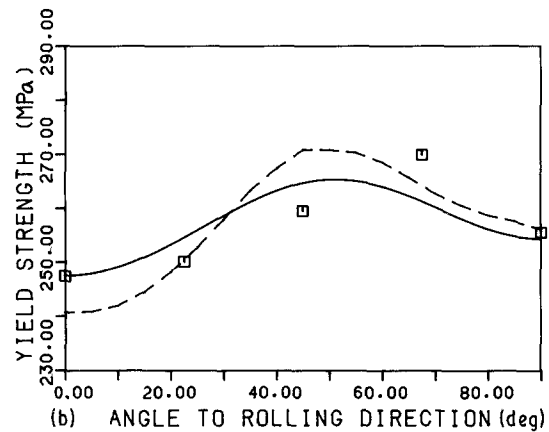
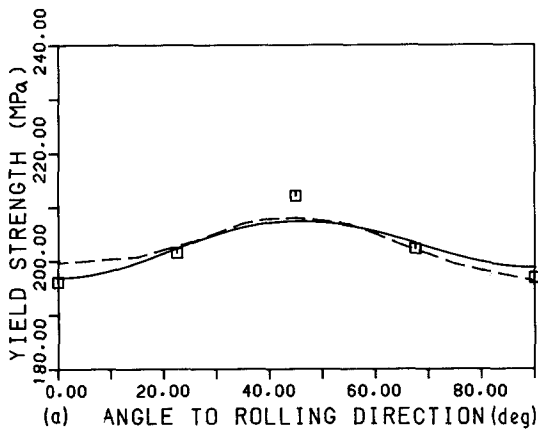


Figure 11 The yield strength as a function of tensile direction for specimen (a) steel A-0, (b) steel A-30A, (c) steel A-30F, (d) steel A-70A, (e) steel B-58A and (f) steel B-58F. (—) Bunge [6], (---) Lee [8], (□) measured.

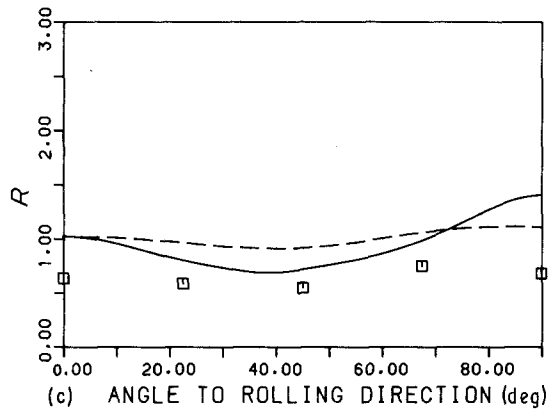
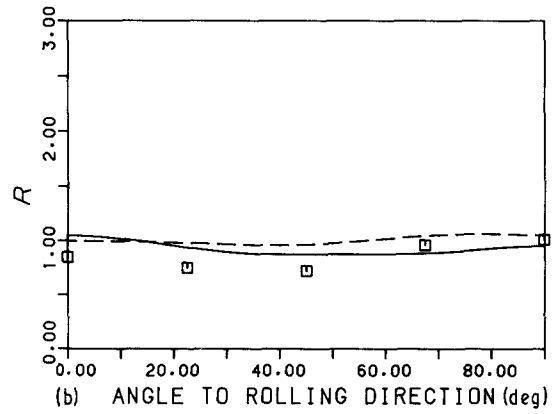
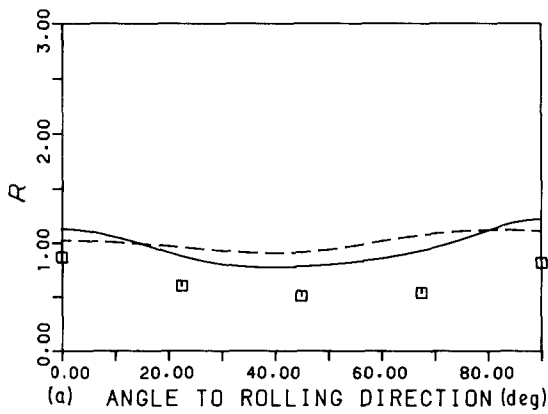


Figure 12  $R$  as a function of tensile direction for (a) Al-0, (b) Al-30 and (c) Al-90 specimens. (—) Bunge [6], (---) Lee [8], ( $\square$ ) measured.

cubic metals the cubic symmetry makes the integral intervals in Equation 21 reduce to

$$0 < \psi_1, \phi, \psi_2 < \pi/2$$

Because  $d\epsilon_w$  and  $d\epsilon_i$  in Equation 21 and  $S_i$  in Equation 23 are calculated when the orientation is given in the form  $(R_1 R_2 R_3) (A_1 A_2 A_3)$ , the orientation  $g(\psi_1, \phi, \psi_2)$  should be transformed to the form  $(R_1 R_2 R_3) (A_1 A_2 A_3)$  using the following relations [6]

$$\begin{aligned} R_1 &= \sin \psi_2 \sin \phi \\ R_2 &= \cos \psi_2 \sin \phi \\ R_3 &= \cos \phi \\ A_1 &= \cos \psi_1 \cos \psi_2 - \sin \psi_1 \sin \psi_2 \cos \phi \\ A_2 &= -\cos \psi_1 \sin \psi_2 - \sin \psi_1 \cos \psi_2 \cos \phi \\ A_3 &= \sin \psi_1 \sin \phi \end{aligned}$$

In this work, numerical calculation of Equations 21

and 24 has been performed at a Euler angular interval of  $5^\circ$ .

### 3. Experimental details

Sheet specimens of commercial purity aluminium, cartridge brass, copper, and steels whose chemical compositions and fabrication conditions are given in Tables I and II were tensile tested to obtain their 0.2% offset yield strengths and the  $R$  values at about 15% strain along the angles of  $0^\circ$ ,  $22.5^\circ$ ,  $45^\circ$ ,  $67.5^\circ$  and  $90^\circ$  to the rolling direction. In order to obtain the orientation distribution functions of the specimens, they were subjected to the pole figure measurement, in which  $\alpha$ -rotation was made from the normal direction ( $0^\circ$ ) to  $70^\circ$  in reflection and from  $40^\circ$  to  $90^\circ$  in transmission, and  $\beta$  rotation from  $0^\circ$  to  $360^\circ$ , at the angular interval of  $5^\circ$ . The (111), (200) and (220) pole figures were measured for the fcc metals and the (110), (100) and (211) pole figures for the bcc metals.

### 4. Results and discussion

#### 4.1. Orientation distribution function

A few examples of the orientation distribution functions obtained for various specimens are shown in Figs 4 to 7.

#### 4.2. Yield strength

Figs 8 to 11 show the yield strength as a function of the tensile direction for the commercial purity aluminium,

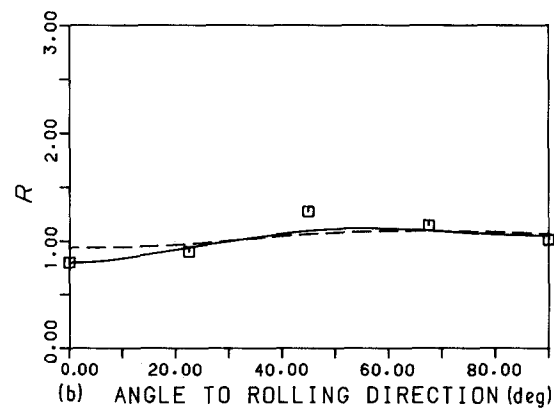
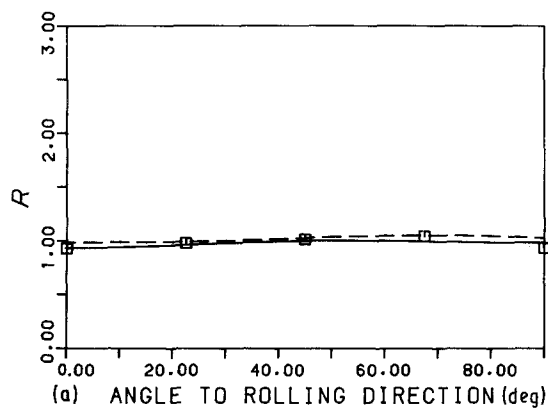


Figure 13  $R$  as a function of tensile direction for (a) brass-0 and (b) brass-70 specimens. (—) Bunge [6], (---) Lee [8], ( $\square$ ) measured.

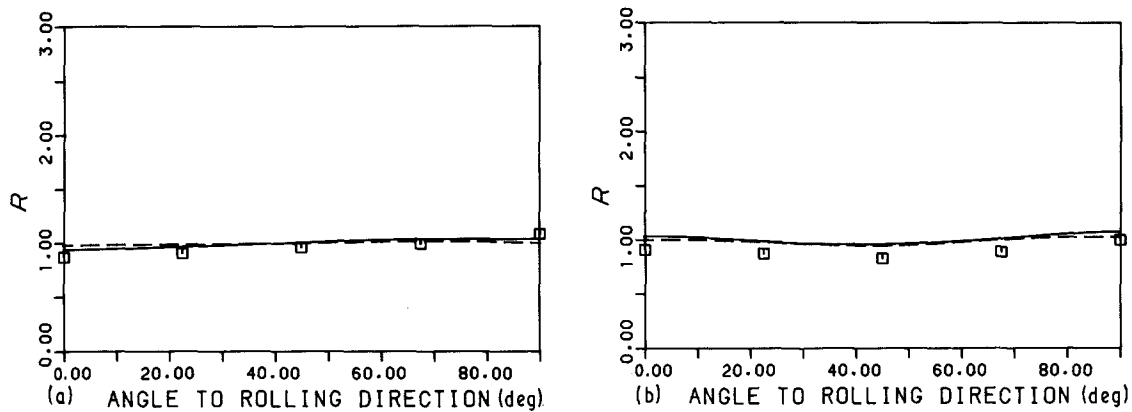


Figure 14  $R$  as a function of tensile direction for (a) Cu-30 and (b) Cu-70 specimens. (—) Bunge [6], (---) Lee [8], ( $\square$ ) measured.

cartridge brass, copper and steel specimens, respectively. The yield strengths calculated from both Equation 13 [6] and Equation 24 [8] are in very good agreement with the measured data. Anisotropy in the yield strength can be influenced by the crystallographic

texture and mechanical fibring. The calculation of the yield strength took no account of mechanical fibring. Therefore, the good agreement between measured and calculated values indicates that the effect of mechanical fibring on the yield strength is negligible.

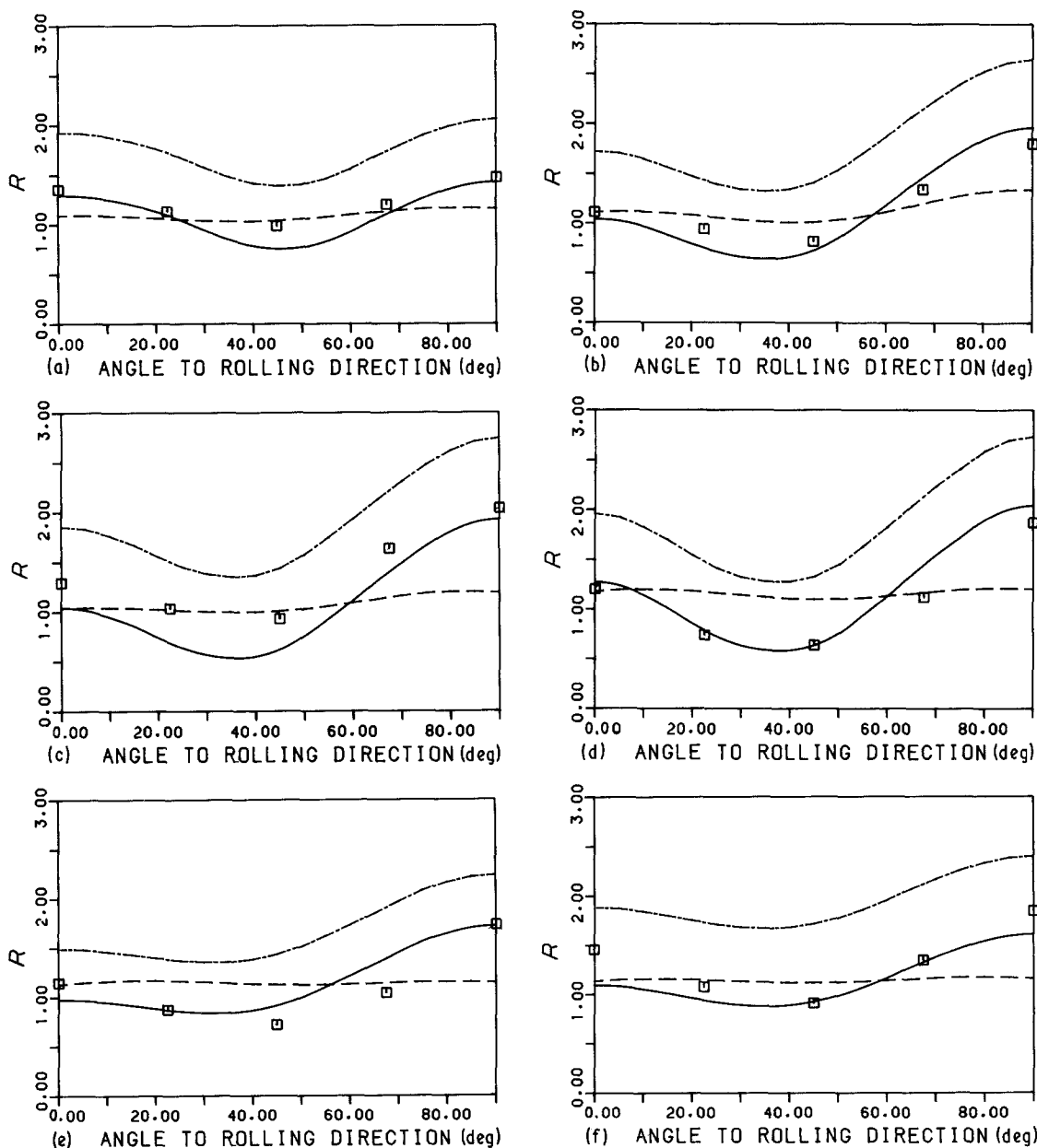


Figure 15  $R$  as a function of tensile direction for (a) steel A-0, (b) steel A-30A, (c) steel A-30F, (d) steel A-70A, (e) steel B-58A and (f) steel B-58F specimens. (—·—) Bunge [6], (---) Lee [7], (—) combined, ( $\square$ ) measured.



TABLE I Chemical composition of steel sheets

Specimen	C	Si	Mn	P	S	Al
A	0.044	–	0.19	0.11	0.11	0.5
B	0.035	0.01	0.19	0.11	0.09	0.24

### 4.3. Plastic strain ratio

The plastic strain ratios or the  $R$  values calculated using Equation 12 [6] and Equation 21 [8] are compared with the measured data in Figs 12 to 15. In calculation of the  $R$  values, the slip systems of  $\{111\}\langle 110\rangle$  and  $\{hkl\}\langle 111\rangle$  were used for the fcc metals and the steels, respectively. For the fcc metals, the calculated values agree reasonably well with the measured data. For the steel specimens, the values calculated from Equation 12 are systematically larger than the measured data, while their variation with the tensile direction agrees very well with the measured values. The values calculated from Equation 21 are in very good agreement with the measured data in their average values, but show a smaller variation with the tensile direction. Therefore, combination of the two methods has been suggested to calculate the plastic strain ratios of the steel specimens, in which the average values are calculated using Equation 21 and the variations with the tensile direction are calculated using Equation 12. Such calculations (combined) yield very good results as shown in Fig. 15. The  $R$  values were calculated using initial orientation distribution functions (at zero strain) and measured at around 15% strain according to ASTM standard. Therefore, it can be argued that the calculated values may be different if changes in texture with tensile strain are taken into account. It has been known that the  $R$  values of cubic metals are not very sensitive to test strain. This problem should be clarified in future studies.

TABLE II Fabrication conditions of tensile specimens

Specimen	Fabrication conditions
Al-0	Commercial purity aluminium sheet annealed at 400°C for 60 min
Al-30	Commercial purity aluminium sheet cold rolled by 30% and annealed at 310°C for 30 min
Al-90	Commercial purity aluminium sheet cold rolled by 90% and annealed at 280°C for 30 min
Brass-0	Cartridge brass sheet annealed at 550°C for 60 min
Brass-70	Cartridge brass sheet cold rolled by 70% and annealed at 300°C for 20 min
Cu-30	Copper sheet cold rolled by 30% and annealed at 350°C for 30 min
Cu-70	Copper sheet cold rolled by 70% and annealed at 350°C for 30 min
Steel A-0	Steel A sheet annealed at 713°C for 2 h and air cooled
Steel A-30A	Steel A sheet cold rolled by 30%, annealed at 713°C for 2 h and air cooled
Steel A-30F	Steel A sheet cold rolled by 30%, annealed at 713°C for 2 h and furnace cooled
Steel A-70A	Steel A sheet cold rolled by 70%, annealed at 713°C for 2 h and air cooled
Steel B-58A	Steel B sheet cold rolled by 58%, annealed at 713°C for 2 h and air cooled
Steel B-58F	Steel B sheet cold rolled by 58%, annealed at 713°C for 2 h and furnace cooled

## 5. Conclusions

1. The variation of yield strength with tensile direction for commercial purity aluminium, cartridge brass, copper and steel sheet specimens fabricated under various conditions could be adequately explained by their crystallographic textures.

2. The measured plastic strain ratios of the fcc metals were in reasonably good agreement with the calculated values.

3. The measured plastic strain ratios of the steel specimens could be very well predicted by combination of the two different methods, in which the one method predicts variation with the tensile direction, and the other the average value.

## References

1. R. L. WHITELEY, *Trans. ASM* **52** (1960) 154.
2. D. N. LEE, *J. Mater. Sci. Lett.* **3** (1984) 677.
3. *Idem*, Theoretical Dependence of Limiting Drawing Ratio, in "Strength of Metals and Alloys", edited H. J. McQueen, J.-P. Bailon, J. I. Dickson, J. J. Jones and M. G. Akben (Pergamon, Oxford, 1985) p. 971.
4. W. F. HOSFORD Jr and W. A. BACKOFEN, "Fundamentals of Deformation", Proceedings of the 9th Sagamore Conference, Syracuse, New York (Syracuse University Press, 1964) p. 295.
5. G. I. TAYLOR, *J. Inst. Metals* **62** (1938) 307.
6. H. J. BUNGE, "Texture Analysis in Materials Science", translated by P. R. Morris (Butterworths, London, 1982) p. 330.
7. D. N. LEE and K. H. OH, *J. Mater. Sci.* **20** (1985) 3111.
8. *Idem*, *J. Korean Inst. Metals* **20** (1982) 586.
9. C. N. REID, "Deformation Geometry for Materials Science" (Pergamon, Oxford, 1973) p. 147.
10. R. W. VIETH and R. L. WHITELEY, 'IDDRG Colloquium', (Institute of Sheet Metal Engineering, London, 1964).
11. M. FUKUDA, *Trans. Iron Steel Inst. Jpn* **8** (1964) 68.

Received 3 November 1987

and accepted 1 March 1988